REPORT DOCUMENTATION PAGE

Form Approved
OMB No. 0704-0188

1. REPORT DATE *(DD-MM-YYYY)*	2. REPORT TYPE	3. DATES COVERED *(From - To)*
08-30-2006	Final	01/01/04 – 09/30/05

4. TITLE AND SUBTITLE
Optimizing Mechanical Properties & Thermal Stability of Age Hardenable Aluminum Alloys through Theoretical Modeling, Alloy Modification & Thermal Mechanical Processing

5a. CONTRACT NUMBER
N/A

5b. GRANT NUMBER
FA9550-04-1-0027

5c. PROGRAM ELEMENT NUMBER
N/A

6. AUTHOR(S)
Starke, E. A.
Shiflet, G. J.

5d. PROJECT NUMBER
N/A

5e. TASK NUMBER
N/A

5f. WORK UNIT NUMBER
N/A

7. PERFORMING ORGANIZATION NAME(S) AND ADDRESS(ES)

University of Virginia
Office of Sponsored Programs
P. O. Box 400195
Charlottesville, Virginia 22904-4195

8. PERFORMING ORGANIZATION REPORT NUMBER

120171-101-GG10584-31340

9. SPONSORING / MONITORING AGENCY NAME(S) AND ADDRESS(ES)
Air Office of Scientific Research
875 North Randolph Street
Suite 325, Room 3112
Arlington, Virginia 22203-1768
Dr Jaimie Tiley/NA

10. SPONSOR/MONITOR'S ACRONYM(S)
N/A

11. SPONSOR/MONITOR'S REPORT

AFRL-SR-AR-TR-06-0382

12. DISTRIBUTION / AVAILABILITY STATEMENT

Approved for public release, distribution unlimited.

13. SUPPLEMENTARY NOTES
N/A

14. This proposal was to design & test an Al-Cu-Mg (Ag) alloy for moderate temperatures (up to 150 degrees C) application. A significant improvement in the creep resistance was primarily pursued in the program through enhancement of the yield strength & the thermal stability of the age-hardenable alloy. Major tasks have been finished as planned: 1) We identified the optimum structures of complex multiple secondary phase precipitates using dislocation slip simulation methods that we developed; focusing on Al-Cu-Mg based alloys with Cu: Mg ratios, vs. determined the omega phase as the main strengthening precipitate phase. 2) We constructed a special thermodynamic database (incorporating the metastable omega phase) to determine the absolute Cu & Mg concentration for optimum chemical driving forces of omega phase nucleation. 3) To control the formation (nucleation) of competing precipitate phases, we developed an effective & efficient approach to characterize effects of alloying elements. The computational tools, combining the state-of-the-art across-scale computational methods from first principles calculations to clustering strain analysis. We demonstrated how trace amounts of Mg & Ag additional catalyze omega phase nucleation & identified Si to be deleterious & that it must be eliminated. 4) We accordingly designed new alloys with compositions: A1-(4 to 5) Cu-(0.4 to 0.6) Mg-(0.4 to 0.06) Ag (wt%)with minimal Si content for the optimum strength & second phase thermal stabilities.

15. SUBJECT TERMS
thermal stability, age-hardenable alloy, optimum structures, thermodynamic database

16. SECURITY CLASSIFICATION OF:			17. LIMITATION OF ABSTRACT	18. NUMBER OF PAGES	19a. NAME OF RESPONSIBLE PERSON
a. REPORT	b. ABSTRACT	c. THIS PAGE			Starke, E.A./Shiflet, G. J.
Unclassified	Unclassified	Unclassified	UL	20	19b. TELEPHONE NUMBER *(include area code)* 434-924-6332/434-982-5653

FINAL TECHNICAL REPORT

GRANT NUMBER FA9550-04-1-0027

DR. E. A. STARKE, PRINCIPAL INVESTIGATOR

DR. G. J. SHIFLET, CO-PRINCIPAL INVESTIGATOR

ABSTRACT

This proposal was to design and test an Al-Cu-Mg (Ag) alloy for moderate temperatures (up to 150 degrees C) application. A significant improvement in the creep resistance was primarily pursued in the program through enhancement of the yield strength and the thermal stability of the age-hardenable alloy. Major tasks have been finished as planned:

1) We identified the optimum structures of complex multiple secondary phase precipitates using dislocation slip simulation methods that we developed; focusing on Al-Cu-Mg based alloys with high Cu:Mg ratios, we determined the omega phase as the main strengthening precipitate phase.

2) We constructed a special thermodynamic database (incorporating the metastable omega phase) to determine the absolute Cu and Mg concentration for optimum chemical driving forces of omega phase nucleation.

3) To control the formation (nucleation) of competing precipitate phases, we developed an effective and efficient approach to characterize effects of alloying elements. The computational tools, combining the state-of-the-art across-scale computational methods from first principles calculations to clustering strain analysis. We demonstrated how trace amounts of Mg and Ag additions catalyze omega phase nucleation and identified Si to be deleterious and that it must be eliminated.

We accordingly designed new alloys with compositions: Al-(4 to 5) Cu-(0.4 to 0.6) Mg-(0.4 to 0.6) Ag (wt%) with minimal Si content for the optimum strength and second phase thermal stabilities

1. Personnel Support

Professor Gary J. Shiflet
Dr. Aiwu Zhu, Research Scientist
Professor Edgar Starke, Jr.
Brian Gable, Ph.D. Student (degree awarded August 2004) Thesis Title:
"The Enhanced Coarsening Resistance and Stability of Omega Precipitates in Al-Cu-Mg-(Ag) Alloys", available by request from University of Virginia Library at URL:
http://www.lib.virginia.edu/questions.html

2. Publications

a. Archival Journal Articles

Gable, B. M.; Shiflet, G. J.; Starke, E. A. "The effect of Si additions on Ω precipitation in Al-Cu-Mg-(Ag) alloys", *Scripta Materialia* (2004), vol. 50, pp. 149-153.

Zhu, A., Gable, B.M., Shiflet, G.J., and Starke, E.A; "Trace Element Effects on Precipitation in Al-Cu-Mg-(Ag,Si) Alloys: A Computational Analysis, *Acta Materialia*, (2004) vol. 52, pp. 3671-3679

Gable, B. M.; Shiflet, G. J.; Starke, E. A., Jr., "Alloy development for the enhanced stability of Ω precipitates in Al-Cu-Mg-Ag alloys" *Metallurgical and Materials Transactions A: Physical Metallurgy and Materials Science* (2006), vol. 37A, pp. 1091-1105.

b. Books/Book chapters/Books edited

Zhu Aiwu, Gary J Shiflet, and Edgar A Starke Jr: "Computational and Experimental Techniques in the Intelligent Design of Age-Hardenable Aluminum Alloys" in Chapter 9 of *Applied Computational Materials Modeling: Theory, Experiment and Simulations*, Springer, 2006, in press

c. Proceeding Article

First Principles Calculations for Alloy Design of Moderate Temperature Age-Hardening Al Alloys", AW Zhu, GJ Shiflet and EA Starke, Jr., pp. 35-44, Aluminium Alloys 2006, Proceedings of the 10th International Conference on Aluminum Alloys, Trans Tech Publications, Switzerland (2006)

3. Participation at Professional Meetings, Conferences and Seminars

"The Design and Development of an Age Hardenable Aluminum Alloy of Moderate Temperature Application", EA Starke, BM Gable and GJ Shiflet, A. Zhu, TMS Charlotte, NC Mar. 17, 2004.

"Trace element effects on Precipitation in Al-Cu- Mg-(Ag,Si) Alloys" Aiwu Zhu EA Starke and GJ Shiflet TMS San Francisco, Feb. 14, 2005.

4. Report of Research Findings

I. Overview

This proposal was to design and test an Al-Cu-Mg (Ag) alloy for moderate temperatures (up to 150 °C) application. A significant improvement in the creep resistance has been primarily pursued in the current program through enhancement of the yield strength and the thermal stability of the age-hardenable alloy. Major tasks have been finished as planned:

4) We have identified the optimum structures of complex multiple secondary (2^{nd}) phase precipitates using dislocation slip simulation methods we developed; focusing on Al-Cu-Mg based alloys with high Cu:Mg ratio, we have determined the Ω phase as the main strengthening 2^{nd} phase and have further understood its high thermal stability due to small amount of Mg and Ag addition using high resolution and analytical TEM.
5) We have constructed a special CALPHAD thermodynamic database (incorporating the metastable Ω phase) to determine the absolute Cu and Mg concentration for optimum chemical driving forces of Ω phase nucleation.
6) To control the formation (nucleation) of competing 2^{nd} phases, we have developed an effective and efficient approach to characterize effects of alloying elements. The computational tools, combining the state-of-the-art across-scale computational methods from first principle calculations to clustering strain analysis and CALPHAD, allow us to identify helpful trace elements and deleterious impurities; applying to Al-Cu-Mg based alloys, we have demonstrated how trace amounts of Mg and Ag additions catalyze Ω phase nucleation and identified Si to be deleterious and that it must be eliminated.
7) We have accordingly designed and developed new alloys with compositions: Al-(4 to 5) Cu-(0.4 to 0.6) Mg-(0.4 to 0.6) Ag (wt%) with minimal Si content for the optimum strength and 2^{nd} phase thermal stabilities.

II. Statement Of Proposal Objectives

The primary design criterion for the base alloy was high creep resistance at and above 150 °C which revolves around selecting the right base alloy and secondary phase(s), and to obtain the optimum strengthening effects and thermal stability through alloying with proper types and amounts of (trace) elements combining with controlled thermal mechanical treatments. This was the major objective of the now ended AFOSR project, which had been about 80% achieved in the last 4.5 years.

We selected Al-Cu-Mg with high Cu:Mg ratio as the base alloy and selected the Ω phase as main strengthening phase in this system[1,2]. As indicated by our dislocation slip simulations, a fine uniform dispersion of Ω plates with $\{111\}_\alpha$ (with small amount of co-existing θ′ with $\{100\}_\alpha$ habits) is desired[3]. For production of the desired precipitate structures we developed a thermodynamic CALPHAD database for the Al-Cu-Mg-(Ag, Si) system[4,5]. The desired phase Ω and the deleterious S-phase as well as the α (FCC), liquid solutions, *etc.* were modeled using data from the quantitative characterization of the phases, measurement of thermal events associated with phase transformations and first principles calculations.[6]. Trace element additions were selected for their formation of the atom aggregates which act as precursors for subsequent precipitation of desired phases. Computational tools, based on first principles calculation (FP), cluster-variation methods (CVM), quasi-chemical models (Quasi-Chem) and computational thermodynamics(CALPHAD), were used to identify the "useful" trace elements and the "harmful" impurities [4,7]. The analysis demonstrated how Cu, Mg and Ag work together to form clusters as the precursors for nucleation of the Ω phase as

partially observed in 3D-atom probe studies[8]. It also indicated Si, a common impurity element in most of aluminum alloys, has a harmful effect on Ω phase formation[9]. The one study in our proposed effort that was not accomplished was to make significant quantities of the newly designed alloy, optimized as Al-4Cu-(0.4 to 0.6) Mg-(0.4 to 0.6)Ag (in wt%) and systematically test in creep conditions at elevated temperatures to validate the alloy selection.

III. Technical Background Used in this Research

Aluminum alloys are classified as heat treatable and non-heat-treatable, depending on whether or not they respond to precipitation hardening[10]. The heat treatable, or more specifically age hardenable, aluminum alloys have been the primary materials of choice for structural components of aerospace systems since about 1930. Application to other transportation tools such as automobiles has gained great momentum recently. However, because of increased performance requirements, conventional aluminum alloys are being challenged by other materials, particularly titanium and carbon-reinforced epoxy-matrix composites. Although nowadays about 60% of the aircraft that operate in a speed less than Mach 2.0 consists of aluminum alloys, the skin temperatures produced at higher Mach numbers prohibit the use of conventional age-hardenable aluminum alloy products. This skin temperature limit corresponds to about 100°C. Since the alternative materials currently in use are expensive and often difficult to fabricate, improving the competitiveness, *e.g.*, enhancing the creep and corrosion resistance, of aluminum alloys has been the topic of the recent research and development efforts. There have been a number of attempts to increase the high temperature performance of aluminum-base materials by dispersion strengthening using rapid solidification or mechanical alloying and powder metallurgy consolidation. However, these materials are expensive and have been shown to have decreasing ductility and fracture toughness with increasing temperature, especially in the temperature range of interest. Therefore, development of high creep resistant aluminum alloys with great corrosion and wear protection will find broad aerospace and transportation application for manufacturing structural components that serve at relatively high temperature and in severely hazardous environments.

Design of new age-hardenable aluminum alloys can be extremely complex. Practically, some primary criteria are set for the most desired properties during the first cycle of the alloy development. A balanced combination must be reached among a variety of the properties including the yield strength, ductility, fracture toughness, stiffness, corrosion resistance, creep-resistance *etc.* during the next test-modification cycles. Aluminum alloys usually have a variety of microstructure features that affect or control those mechanical properties in different ways. These features include the grain structures, dislocations patterns (sub-grain structures), constituent particles, dispersoids, equilibrium secondary phase precipitates and strengthening phase precipitates as well as their interactions. The fine dispersoids (0.01-0.2 μm), formed by transitional metal elements during ingot preheating, are at least partially coherent with Al matrix and can act as recrystallization barriers. The large incoherent constituent particles (1-30 μm in diameter), formed through the liquid-solid eutectic reactions by impurities during solidification or casting process, can act as void nucleation sites during deformation and hence reduce the fracture toughness. The subgrain structures have small and variable impacts on the strength and strain localizations, but more significantly on the 2nd phase precipitation. Equilibrium 2nd phase precipitates, usually incoherent, coarse and heterogeneously distributed, have little strengthen effect. They are primarily formed at grain boundaries (GBs) may lead to formation of GB precipitate free zones (PFZ) and hence nurture the strain localization and lower the fracture toughness. The grain structures may be controlled to a large extent by adding certain elements to form fine dispersoid phases combining with suitable thermo-mechanical processing[11]. The grain structure effects and the grain-texture induced anisotropy have been

extensively studied and can be assessed based on well-developed theories. As far as the strengthening effect and work hardening are concerned, the major factor is the strengthening 2nd phases that are formed during the aging treatment. They are usually coherent or semi-coherent and homogeneously distributed inside the grains. To some extent, the solute atoms remaining in the matrix function in the similar way to those 2nd phase particles, and hence they can correspondingly be evaluated. Therefore, to reach the primary alloy design goal of high creep resistance, the 2^{nd} phases and their precipitates structures must be concentrated.

Due to economic considerations, alloy design and development can no longer be performed using the purely empirical, trial and error approach that has been dominate over the past 100 years. Modeling and simulation, in conjunction with experiments, can be employed to improve the efficiency of alloy design, optimizing processing and manufacturing operations. This approach can greatly reduce the time associated with alloy development and the generation of the knowledge base required for insertion of new materials into aerospace systems. Our research and development approach that resulted from this program was aimed at obtaining a high-strength, thermally stable aluminum-based alloy with corrosion and wearing protection that would be suitable for moderate temperature applications up to 150°C in severely hazardous environments. The fuselage of a Mach 2.2-2.4 aircraft is an example. Ultimately, this research was to provide an example of streamlined alloy design based upon the marriage of theoretical metallurgical principles, calculated phase diagrams and experimental alloy design and processing. An outline of our program is represented in **Figure 1**.

The first step was to select a base alloy system that offered promise for obtaining the desired microstructure and properties. After an extensive literature search and examination of empirical data, we selected the Al-Cu-Mg system for our base system. In order to identify the optimized precipitate structure and morphology, our research team developed a dislocation-slip simulation method[3,12]. In combination with a quantitative microstructure characterization procedure, we were able to evaluate superposition of the strengthening effects of precipitates with different volume fractions, sizes, shapes (aspect ratio) and orientations with respect to the Al-matrix. This allowed us to find the optimized precipitate-structure for maximum strength. Regarding the Al-Cu-Mg-Ag-X system, we were concerned with Ω (Al_2Cu), a plate-like phase with a $\{111\}_\alpha$ habit plane, $\theta'(Al_2Cu)$ plate-like phase with a $\{100\}_\alpha$ habit-plane, and S (Al_2CuMg) a rod-like phase oriented along the $<210>_\alpha$ direction. These three phases may co-exist in many Al-Cu-Mg-Ag alloys under conventional processing conditions. The rod-like S or S′ phase is less effective in the strengthening, possibly due to its particular orientation which results in relatively small obstacles to dislocation motion on $\{111\}_\alpha$ slip planes. Our dislocation-slip simulations revealed that for optimal strength, a fine uniform distribution of Ω plates with small amount of θ' is desired.

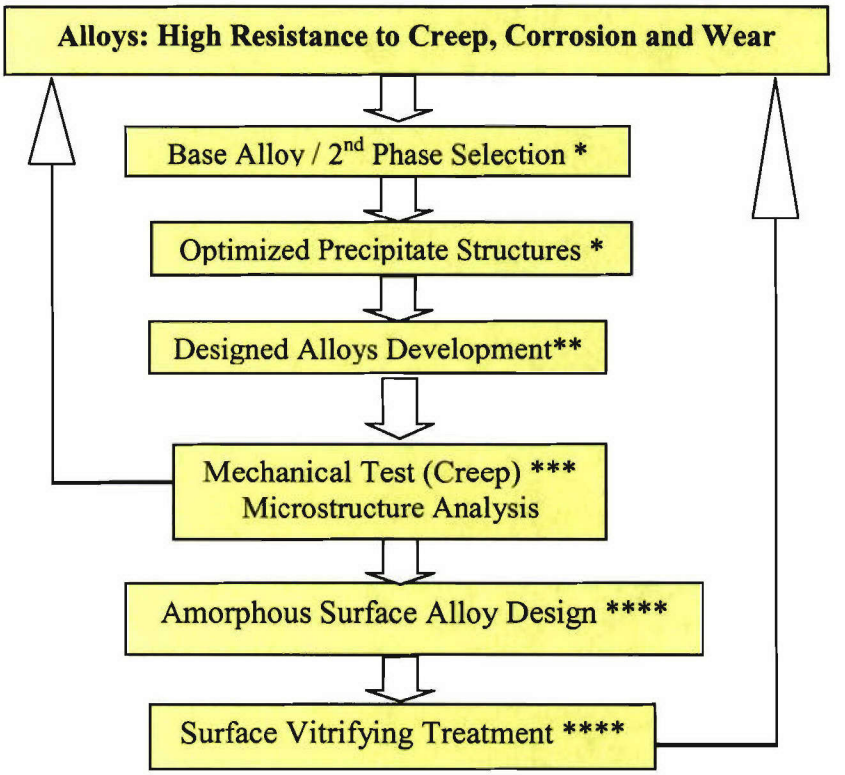

Figure 1 Project Flowchart: *— finished; **— 80% finished; ***— 10% finished; **** — new

The Al-Cu-Mg-(Ag) System: The strengthening precipitates, especially the $\{100\}_\alpha$ Al_2Cu phase (θ'/θ), in the Al-Cu-Mg-X 2XXX alloy system are more thermally stable at moderate temperatures than those present in the Al-Zn-Mg-X 7XXX or the Al-Si-Mg 6xxx alloy systems. The addition of small amounts of Ag, on the order of 0.4 $^{wt}/_o$, to Al-Cu-Mg-X alloys with high Cu:Mg ratios (*e.g.* 10:1 $^{wt}/_o$) has been shown to significantly enhance the age hardening response over that of a similar ternary alloy (c.f. [13]). The marked gain in strength results from the formation of a uniform dispersion of a hexagonal plate precipitate with a $\{111\}_\alpha$ habit plane, designated Ω. Several detailed studies have indicated that the internal crystal structure of the Ω plates is quite similar to that of equilibrium θ [14,15,16,17,18]. As will be described later, we have assessed the validity of this assumption.

It has been shown that Ag facilitates Ag-Mg clusters that in turn act as nucleation sites for the Ω phase[19,20]. Detailed atom probe and high resolution Z-contrast microscopy have revealed that Ag and Mg are present at the coherent interfaces between the Ω plate and the enveloping aluminum matrix[Error! Bookmark not defined.,19,20]. Two prominent factors that jeopardize the fine uniform distribution of Ω plates in the quaternary alloys have also been identified. The long-term stability of the Ω plate is sensitive to the presence of S-phase precipitation (Al_2CuMg). If the alloy composition lies within the equilibrium ($\alpha + \theta + S$) phase field the existence of S-phase will create chemical potential (μ) gradients in Mg. Essentially the presence of equilibrium S-phase limits the Mg available for the coherent interfaces of the Ω plates. Similarly, several studies have illustrated Ag segregation to S-phase in this class of quaternary alloys[20,21]. The presence of S-phase is deleterious to the stability and coarsening resistance of Ω plates due to the fact that the Ω plates may only exist with Mg and/or

Ag at the coherent interfaces. The first goal was to design a quaternary alloy that lay within the (α + θ) phase field for a wide range of desirable temperatures. Therefore, we required a thorough understanding of phase space for both the Al-Cu-Mg ternary and the Al-Cu-Mg-Ag quaternary Al-rich alloys. Once within the ($\alpha + \theta$) phase field the driving force for coarsening of the Ω plates must be substantially reduced in order to maintain a fine uniform and thermally stable distribution.

Thermal Stability of the Desired Precipitate Structures: The coarsening behavior of the Ω plates in Al-Cu-Mg-Ag was studied in our lab [6,Error! Bookmark not defined.]. The coarsening or thickening rate is slower when the thickness of Ω-plates is less than ~ 13nm. This may be attributed to the inability to form the misfit compensating *in-situ* dislocations at the edge interface between the plates and the matrix. The vacancy (dilation) strain associated with the (–9%) misfit between the single ½ unit cell high Ω-plates and 2 $\{111\}_\alpha$ plane spacing makes the nucleation of thickening ledges difficult, particularly during the coarsening stage where the driving forces will be much lower than during growth. When the plates are thicker than the critical value, acceleration in thickening occurs due to the relaxation of the strain field with the formation of the misfit dislocations. Another important finding is the trace element segregation in the broad interfaces of Ω plates.

More generally, there are two issues for the thermal stability of a precipitate structure containing more than one 2nd phase – phase coarsening and phase competition from other phases. Coarsening of a single 2nd phase is thermodynamically attributed to the tendency for decreasing the total interfacial energy between the 2nd phase and the Al-matrix. The interfacial energy may consist of the chemical energy, as described by the bond-breaking model, and the associated strain energy. Trace element additions may have two possibly "useful" ways of partitioning: either segregating at the interfaces or being soluble in the 2nd phase. The former alters the chemistry of the interfaces, *e.g.* Ag layers observed by Z-contrast HRTEM, possibly leading to a lower interfacial energy. The partitioning into the 2nd phase, like the Zn-partitioning in T_1 phase[22], changes the lattice constants and may hence modify the misfit strain. It was also shown that Ag segregates to S phase in an Al-Cu-Mg-Ag alloy. On the other hand, different from the simple alloys in the two-phase field, the coarsening behavior of higher-order alloys like the Al-Mg-Cu-(Ag)-(Si)-X system containing more than one 2nd phase (like Ω , θ' and S) is also affected by the competition from other 2nd phases for the solute Cu, Mg and/or Ag that they share. For example at service temperatures (<150°C) usually lower than aging-treatment temperatures >200°C, the driving force for formation of S-phase will inevitably become significant. The formation of S-phase consuming the solute Mg and Ag, that are stabilizers for Ω, and Cu in the Al matrix and, hence, make both θ' and Ω particles less stable leading to potential dissolution. Therefore, our objective here was not only to lower the coarsening rate of Ω and θ'-plates but also to prevent the S-phase from jeopardizing the stability of the Ω plates.

IV. Principal Achievements

The following section describes the main achievements we have made.

1. Fundamental properties of the 2nd phases

Combination of the experimental techniques and the computational methods were employed to determine the fundamental properties of the 2nd phases that are usually difficult to measure because of their low volume fractions and small sizes.

1.1 Crystalline Structures

The very early XRD study by Perlitz and Westgren (PW)[23] suggested S (Al_2CuMg) phase in Al-Cu-Mg system has an orthorhombic structure with unit cell dimensions a=0.4 nm, b=0.923 nm, and c=0.714 nm, space group *Cmcm*, containing 16 atoms in the ratio Al:Cu:Mg=2:1:1. However since then, there has been extensive investigation that yielded varied results suggesting similar but different models (*c.f.*, references in [[24]]). One of the most recent HRTEM and microanalysis studies [24] confirmed the symmetry, chemical composition and the lattice parameters of the PW crystalline structures except the atomic site-positions. However, comparison between the recorded images with simulations from different models indicated that the match between experiment and simulation could be improved further from the PW model by an exchange of Mg and Cu (referred to as the RaVel model) atomic sites; the intensity distribution as shown in **Figure 2** also support this point.

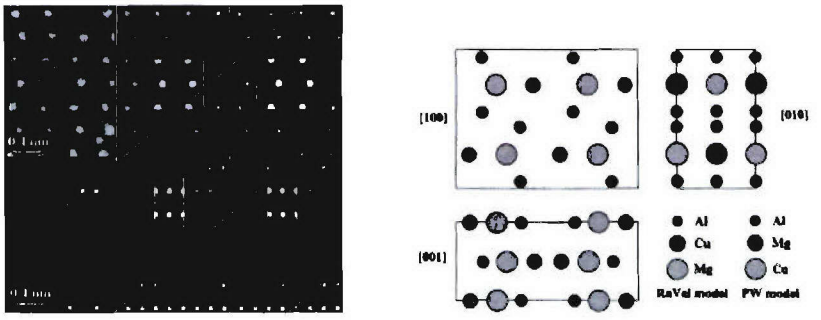

(a) (b)

Figure 2 (a) Quantitative analysis of HREM images along [100]S (first row) and [010]S (second row). First column: as-recorded images; second and third columns: processed images with insets showing image simulations based on two different models, PW and RaVel, respectively. (b) Schematic drawing of the S-phase crystal structure; the difference between the PW and RaVel model is indicated[24].

First Principles (FP) calculation[25] was used to compare the energetics of the corresponding crystalline structures[26]. The calculation, verifying a similar study[27], showed that the original PW model leads to a formation enthalpy of -0.210 eV/atom while the exchange of Cu and Mg in internal atomic coordinates, as suggested by in [24], yielded a positive formation enthalpy of +0.289 eV/atom. By neglecting the entropy contribution (mostly from lattice vibration), this indicates that the PW model is more reasonable.

Several crystal structures have also been proposed for the Ω phase. Auld suggested a monoclinic structure[28] while a widely accepted structure[29,30,31] is orthorhombic with a Fmmm space group. Based on analysis of convergent-beam electron diffraction patterns, Garg and Howe[32] advocated a tetragonal structure (I4/mcm) that is a metastable $\{111\}_\alpha$ variant of the equilibrium θ phase. The first principles calculations have ruled out the monoclinic structure because of its positive formation enthalpy[33]. The energetic difference between the tetragonal and orthorhombic structures is negligible, as shown in Table 1. It shows both the tetragonal structure and the orthorhombic one have the formation enthalpies that are close to the equilibrium θ. **Figure 3** illustrates the orientation relationship between the proposed tetragonal structure of Ω and Al matrix [1].

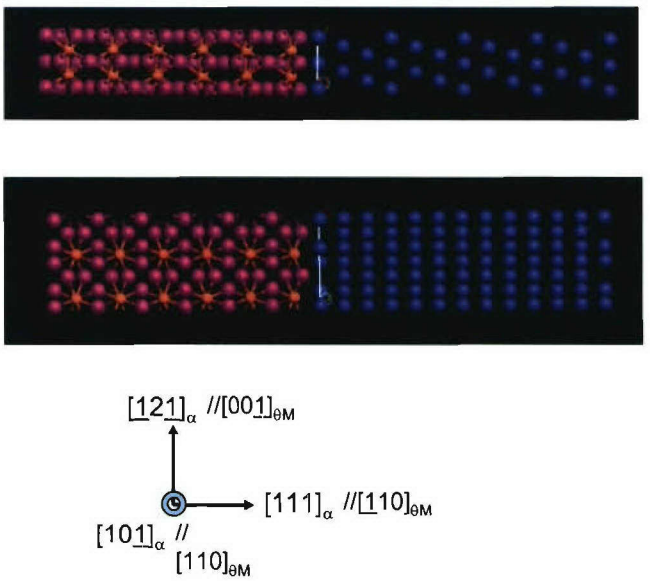

Figure 3 Supercell construction of interfacial structure between Ω<001> and Al<111>. The top is the projection on YZ-plane and the middle is on XZ-plane. The bottom shows the orientation match between the two phases.

Table 1 VASP Calculated Formation Enthalpies of Proposed Crystal Structures for Ω and θ phases as compared with that of θ obtained from optimization using thermodynamic models.

Phase	Proposed structure	ΔH, eV/atom
θ	Tetragonal (I4/mcm)	-0.168
Knowles' Ω	Orthorhombic(Fmmm)	-0.167
Garg & Howe's Ω or θ_m	Tetragonal (I4/mcm)	-0.169
θ as modeled in COST507 etc.	2 sub-lattice ordered compound with composition Al2-Cu	-0.164

1.2 Elastic Constants

Table 2 Elastic constants calculated using VASP based on the local density approximation and obtained from experiments at room temperature for some elementary crystals and 2nd phases

Phase	Structure	Elastic Constants, 10^{10} N/m^2	
		Calculated	Experimental
Al	FCC	C_{11}=9.30, C_{12}=6.38, C_{44}=3.13, B=7.35	C_{11}=10.8 C_{12}=6.13 C_{44}=2.85,B=7.2
Cu	FCC	C_{11}=17.9,C_{12}=12.4,C_{44}=8.03, B=14.27	C_{11}=16.84,C_{12}=12.14,C_{44}=7.54,B=13.7
Ag	FCC	C_{11}=10.93,C_{12}=8.39,C_{44}=3.78, B=9.24	C_{11}=12.4,C_{12}=9.34,C_{44}=4.61,B=10.36
Mg	HCP	C_{11}=5.39, C_{33}=4.78, C_{12} =2.39, C_{13}=3.26, C_{44}=1.75	C_{11}=5.64, C_{33}=5.81, C_{12} =2.32, C_{13}=1.81, C_{44}=1.68
θ'	Tetrahedral	C_{11}= 19.24 , C_{33} = 15.62, C_{12}=2.91, C_{13} = 6.54, C_{44}=8.35, C_{66} = 4.36	n. a.
Ω/θ/θ_m	Tetrahedral	C_{11}=18.72, C_{12}= 5.59, C_{13} = 5.36 C_{33}=18.30, C_{44} = 3.68, C_{66}= 6.27	n. a.
S	Orthorhombic	C_{11}=14.5,C_{22}=15.3,C_{33}=14.3,C_{12}= 3.0, C_{13}=6.6,C_{44}=5.3,C_{55}=7.3,C_{66}=3.3	n. a.

Because of their low volume fractions and small sizes, elastic constants of the 2nd phases are difficult to measure experimentally, *e.g.*, by means of ultrasonic techniques. The second order elastic constants of the crystalline solids may be defined and calculated according to the variation in the energy from its optimized lattice structure as

$$C_{ijkl} = \left(\frac{\partial E}{\partial \underline{\varepsilon}_{ij} \partial \underline{\varepsilon}_{kl}}\right)_{E=E_{\min}} \quad i,j,k,l = 1,2, \text{ or } 3 \tag{1}$$

where E denotes the total energy associated with the deformation and $\{\underline{\varepsilon}_{ij}\}$ the strain tensor. Using FP calculation, one may obtain some reasonable information as verified by comparing calculated values with those experimentally measured at the room temperature for known crystal structures, as shown in Table 2. The calculated elastic tensors for the θ′, Ω, θ_M, θ and S phases are listed there.

1.3 Thermal Stability of Ω phases

To achieve a high creep resistance, among all the 2nd phases, Ω phase is desirable for its superior thermal stability; the Ω plates reach thickness lower than 6 nm after 100h exposure at 200°C, after which there is no detectable change in average thickness [34,35] for more than 150 days. The Ω phase structures can thus be retained at up to 200°C without significant coarsening. The high coarsening resistance of Ω plates can be attributed to a prohibitively high barrier to migrating ledge nucleation in the strong compressive strain field normal to the broad faces of the plates. As a result, the fine and uniform dispersion of the Ω plates can ensure the superior yield strength.

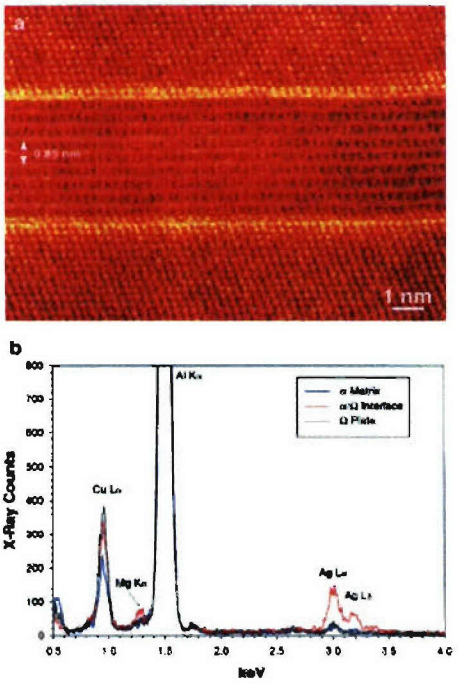

Figure 4 (a) Atomic resolution Z-contrast image of an Ω plate in Al–4Cu–0.3Mg–0.4Ag (wt. %). ST 525°C 1 h, WQ, 200°C 100 h. The electron beam is close to <110>. (b) EDS spectra obtained from the adjacent matrix, the (001)‖(111) interphase boundary and within the Ω plate [Error! Bookmark not defined.].

A high resolution Z-contrast TEM combining with EDS study revealed more details for the enhanced coarsening resistance of the Ω plates[Error! Bookmark not defined.]. Figure 4(a) shows the

micrograph of a 4 unit cell thick Ω plate in an Al-4Cu-0.3Mg-0.4Ag aged at 200°C for 100 h. Two atomic layers of enhanced intensity at the plate/matrix $(001)_\Omega \| (111)_\alpha$ interface indicates atomic segregation. This is in contrast to the monatomic layer reported by Reich et al.[36]. The layers of enhanced intensity within the plate parallel to the habit plane are separated by 0.424 nm and correspond to layers enriched in Cu. Figure 4(b) shows EDS spectra obtained from the matrix, the $(001)_\Omega \| (111)_\alpha$ interphase boundary and from within the plate. The interfacial segregation was found to contain both Ag and Mg.

2. Production of Desirable 2nd Phase(s) and Precipitate Structures

The goal of the alloy design in this aspect was to produce a fine and uniform dispersion of the desirable 2nd phase and at same time to avoid or suppress the formation of those 2nd phases that consume the solutes and hence are deleterious. From the perspective of precipitation kinetics, the formation of a 2nd phase can be distinguished in three stages: nucleation, growth and coarsening. Usually, chemical potentials of the solutes have a great drop during nucleation and early stage of the growth, leading to diminished chemical driving forces for the 2nd phases that are composed with those solute atoms[37]. It indicates that for multiple 2nd phases that share the solute contents, it is their relative nucleation rates that decide the formation preference of one particular 2nd phases over the other.

Technically there are approaches that could be considered to enhance the nucleation rates of desired phases and the same time to suppress the undesired phases: 1) composition optimization to adjust nucleation driving forces for these concerned phases; 2) trace element additions or elimination of deleterious impurities; 3) introduction dislocations or dislocation jogs (subgrain boundaries) as the heterogeneous nucleation sites by cold-working prior to aging treatment like T8 temper; 4) refining grain structures; 5) optimization the quenching rates to adjust the vacancy density and thereby, to enhance the solute diffusivities; 6) to adjust conditions of the aging treatments like temperature, time and sequences *etc.* Applying to the Al-Cu-Mg based alloys, the tactics 1) and 2) are decisive. For the composition optimization, we resorted to phase diagrams and more quantitatively to the CALPHAD databases; for trace element effects, we have developed an efficient and effective approach to analysis of clustering formation.

2.1 Phase Diagrams and Thermodynamics Models

Experimental investigations of Al-Cu-Mg alloys with a Cu:Mg ratio>1 that lie in the Al-rich corner of the phase diagram indicate that the stable 2nd phases are θ (Al_2Cu), S (Al_2CuMg) and T ($Al_{32}(CuMg)_{49}$)[38]. For Al-Cu-Mg with high Cu:Mg ratio, a CALPHAD database has been optimized by experimental assessment of the phase boundaries, as shown in **Figure 5**, using long-term aging treatments[5].

We have verified the discovery by Ringer *et al.* of Ag partitioning to the S-phase precipitates, as shown in **Figure 6**.

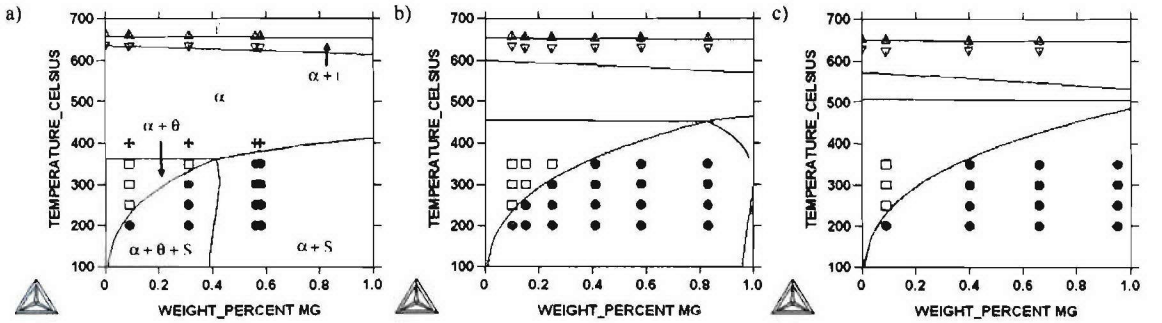

Figure 5 Series of calculated a) 1.0wt% Cu, b) 2,5wt%Cu and c) 4.0wt%Cu isopleth sections for the Al-rich corner of Al-Cu-Mg systems based on an optimized database. The closed circles represent S-phase precipitation, the open squares indicate that no S-phase was observed, the open crosses signify complete solid solutions and the open triangles are the average heating and cooling values for the thermal events as measured by DTA.

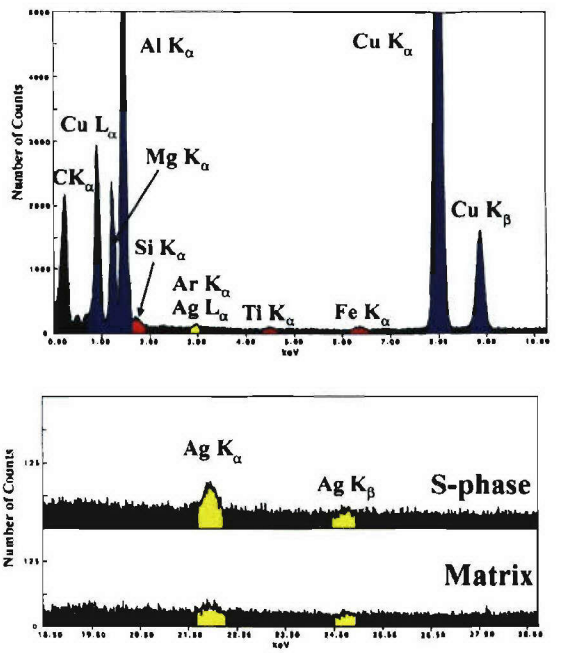

Figure 6. a) Representative EDS spectra collected from within a S-phase precipitate aged at 250°C for 1000h. b) High-energy regime of EDS spectra illustrating the partitioning of Ag to the S-phase precipitate relative to the surrounding matrix.

The metastable phase Ω, possessing similar chemistry and crystal structure to equilibrium θ, has not been modeled. As shown in Table 1, both the tetragonal and the orthorhombic structures of the Ω phase have formation enthalpies that are essentially the same as the θ phase. According to the CALPHAD database, the formation enthalpy of the equilibrium θ phase is -164 meV/atom. Although the entropy related term of Ω phase is not known, it may be thermodynamically treated as equivalent to the θ phase. Solubility of Ag[39] in Ω is negligible and there is no report on Si solubility. Ω-phase can thus be treated as a two sublattice ordered compound, similar to that of θ in the databases. Modifying the θ parameters according to these calculated formation enthalpies (-0.169 eV/atom) of the Ω phase yields little difference in the phase equilibria as shown in **Figure 7**. Calculated phase diagrams of Al-Cu-Mg, Al-Cu-Mg-0.005Si and Al-Cu-Mg-0.005 Ag at 600 K are

given in **Figure 7**. This figure shows that this amount of Si addition has little effect on the phase equlibria while the same amount Ag additions shift the boundary between the (FCC+Ω) field and the (FCC+ Ω +S) field to a little higher Mg concentrations. For the 2nd precipitate nucleation, as shown in **Figure 8**, the chemical driving forces for Ω phase have minimal reduction with addition of either Si or Ag of that amount, but there are obvious greater reductions for S phase with Ag addition than Si.

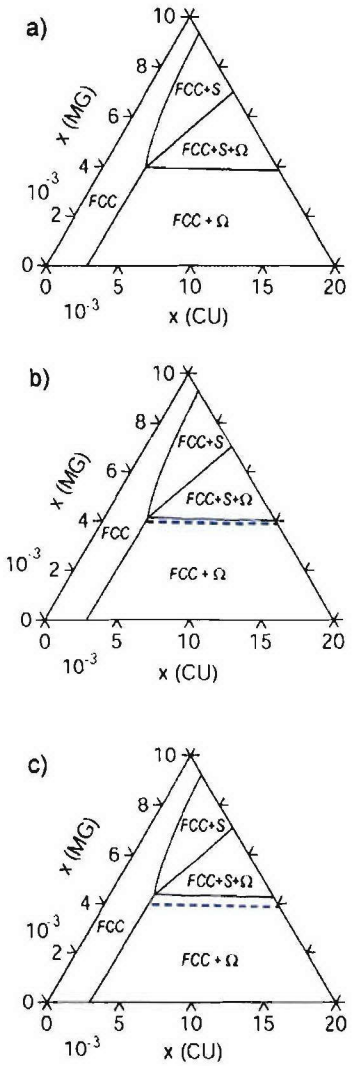

Figure 7 Calculated phase diagrams: isothermal sections at the Al-rich corner at 600 K for a) Al-Cu-Mg, b) Al-Cu-Mg-0.005Si and c) Al-Cu-Mg-0.005Ag. The dotted lines in b) and c) denote the positions of the corresponding phase boundaries for the ternary Al-Cu-Mg system. The units are molar fractions.

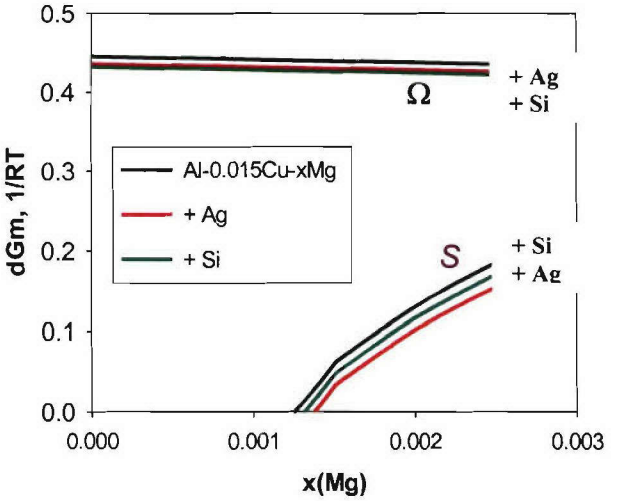

Figure 8. Calculated chemical driving forces (reduced by RT) for nucleation of Ω and S phases at 600 K

It can be concluded that trace amount of Ag and Si have impacts, varying from marginal to noticeable, on the nucleation chemical driving force for certain 2nd phases. However, these impacts are not as significant as to determine the nucleation preferences for the alloys with given compositions close to the phase boundaries[1].

3. Controlled Nucleation: Trace Element Effects

Principally, as a result of atomic interactions, the individual clusters (clustering) or co-clusters (short-range-ordering) between elements can be formed locally in an otherwise homogeneous solid solution. So questions arises as to what elements can form clusters and what clusters work as precursors for a particular 2nd phase. Difficulties for characterization of trace element effects are obvious due to the extremely small sizes and trace amount. For characterization of the clusters, 3D-atom probe provides a useful way to observe remarkably intensive solute clustering but clusters with less intensity are mostly beyond the state-of-the-art microscopy techniques.

Answering these two questions, we developed computational tools to illustrate effects of different trace elements and further to identify what elements are helpful or harmful for the formation of the desirable phases.

3.1 Clustering: FP-CVM Prediction[7]

The cluster-variation-method (CVM) based on first principle total energy calculation (FP-CVM) has been established to predict clustering tendency of solutes in Al matrix. The cluster energetics are obtained via first principle calculation packages like CASTEP[40] or VASP[41] that are based on the density functional theory with the plane-wave pseudopotential method. The ultrasoft pseudopotentials are set globally while GGA-PBE[42]— a non-local gradient-corrected exchange-correlation functional -- is chosen for each individual atom (GGA denotes "generalized gradient approximation"). The configuration entropy of an FCC solid solution is formulated based on the cluster variation method under the tetrahedron approximation (T-CVM) where only 1st neighbor atomic interaction is considered.

For pairing effects in binary systems the chemical ordering at local crystal structures, reflected in either clusters or the atomic aggregates in the solid solution can be demonstrated using the Warren-Cowley parameter $y_{ij} = 1-Y_{ij} / X_iX_j$. This "kinetic" type of parameter effectively

indicates the atomic distribution deviation that clusters will have from random solutions that are generally assumed as the ideal supersaturated states following quenching. A negative value of y_{ij} represents pairs between i and j are favorable in the solid solution. As simple extensions to atomic pairing, similar parameters can be introduced to represent "triangle" cluster formation tendency $z_{ijk} = 1\text{-}Z_{ijk}/X_iX_jX_k$ for the corresponding triangle $\{ijk\}$ and $u_{ijk} = 1\text{-}U_{ijk}/X_iX_jX_kX_l$ for tetrahedrons $\{ijkl\}$.

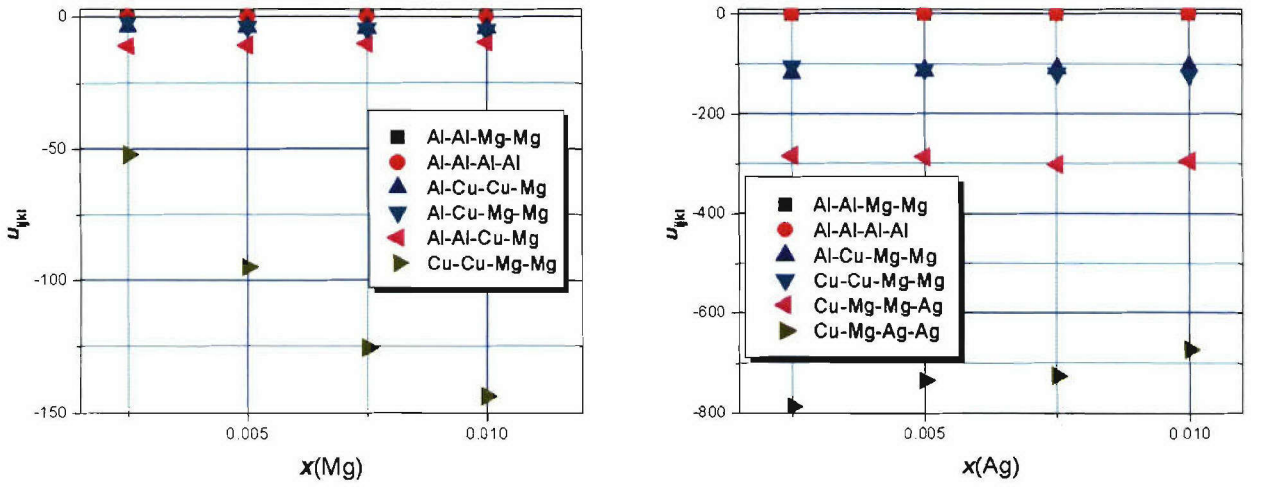

Figure 9 FP-CVM calculated variation of $\{u_{ijkl}\}$ parameters of (a) Al-0.02Cu-xMg with x(Mg) and (b) Al-0.02Cu-0.005Mg-xAg with x(Ag) at 600 K (concentration in atomic fraction).

As shown in **Figure 9**(a), in ternary Al-0.02Cu-xMg (x=0.0025-0.01) alloys at 500 K, the parameters u_{ijkl} are positive (close to 1.0) for the tetrahedron Al-Al-Mg-Mg *etc.* and are neutral approximately at 0.0 for Al-Al-Al-Al. Very negative u_{ijkl} values indicates strong clustering tendency of Cu-Cu-Mg-Mg, Al-Al-Cu-Mg and Al-Cu-Cu-Mg *etc.* With an addition of Ag to Al-0.02Cu-0.005Mg alloys, Cu-Mg-Ag-Ag, Cu-Mg-Mg-Ag, Al-Cu-Mg-Ag *etc.* are much favorable in terms of tetrahedron configurations, as shown in Figure 9(b) for the situation. This leads to favorable Cu-Mg, Mg-Ag and Cu-Ag pairing. These agree well with the observation of the field-ion microscopy based AP and TEM experiments[20,19].

3.2 Clustering: CALPHAD Based Quasi-Chemical Model[4]

Corresponding to the sub-regular model for solutions, a quasi-chemical model for a higher order system with n components has been constructed. For a sub-regular solution, the Gibbs energy ΔG_{mix} of mixing can be written in a Redlich-Kister-Mugianu equation[43] with reference to the purely elemental phases. The heat of mixing depends on the composition $\{x_i$ (molar fraction of component i)$\}$ and temperature T,

$$\Delta H_{mix} = \Delta G_{mix} - T\frac{\partial \Delta G_{mix}}{\partial T}\bigg|_{P,x_i} \qquad (2)$$

where the interaction parameters for ΔG_{mix} can be retrieved from the corresponding CALPHAD databases.

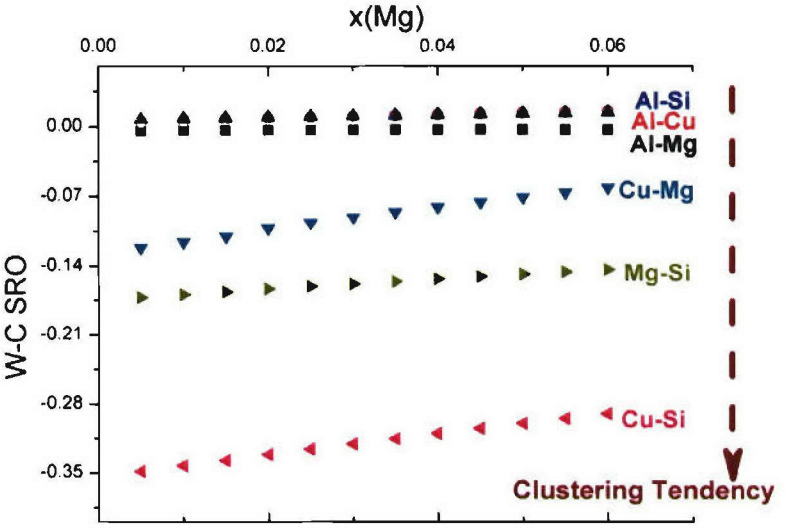

Figure 10 Warren-Cowley SRO parameters for each element pair in Al-0.0175Cu-0.005Si solid solutions at 600 K calculated by CALPHAD based Q-Chem Model.

Figure 10 illustrates the Warren-Cowley parameters calculated for each pair of elements in Al-0.0175Cu-xMg-0.005Si solid solutions at 600 K (x=0.005 to 0.06). Dominant co-clustering occur between Cu-Si, Mg-Si in the Al-0.0175Cu-xMg-0.005Si. Although there is no direct observation of the cluster formation, the deleterious effect of a Si-addition on Ω precipitation can be attributed to the strong tendency of Mg-Si and Cu-Si co-cluster formation that consumes Mg and Cu from solution, leading to the decrease in Cu-Mg clusters that are necessary for Ω formation as will be discussed more in the next section.

3.3 STRAIN ENERGY ANALYSIS[4]

The strain energy analysis of these types of clusters in Al solid solutions may provide information as to which clusters or co-clusters will assist in the formation of the desired plate-like precipitates having specific habit planes[44]. Under approximation of minimal thickness, a coherent platelet-like cluster within the matrix may be treated similarly to an epitaxial layer upon a substrate as described in Hornstra-Bartels Model[45,46]. Figure 11 illustrates the orientation dependence parametric plots of the epitaxial strain energy for some clusters in Al.

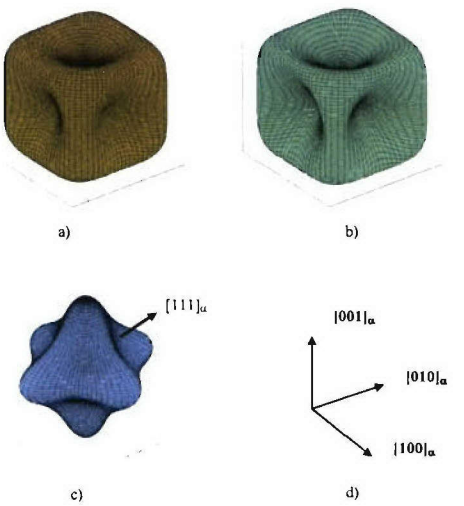

Figure 10 The parametric plot of the orientation {*hkl*} dependence of epitaxial strain energy (under minimal thickness approximation) caused by embedding a platelet-like FCC-A1 cluster in an Al-matrix oriented with respect to the Al-cubic coordinates. a) Cu; b) (postulated) FCC Mg; and c) a CuMg3-FCC mixture. Insert d) indicates the cubic coordinates of the FCC-matrix.

Eshelby's inclusion model[47,48] model can be utilized to more precisely account for the elastic strain or displacement associated with embedding of the coherent clusters in the matrix. Since both matrix and the plates have cubic crystalline structures, the associated strain energy has a minimum with $\xi = \{100\}_\alpha$ and maximum with $\xi = \{111\}_\alpha$, or vice versa. Therefore, only $\{100\}_\alpha$ and $\{111\}_\alpha$ platelets will be considered. The calculation results of the Eshelby's inclusion energies are consistent with the epitaxial energy calculations. It shows that the Cu-FCC plate-like clusters have the highest strain energy when they are parallel with $\{111\}_\alpha$, and the lowest strain energy when parallel with $\{100\}_\alpha$. This explains the formation of Cu plate-like clusters on the $\{100\}_\alpha$, which are experimentally observed in Al-Cu using 3D-AP. The hypothesized Mg FCC structure and Ag-3Mg "FCC" superstructure are similar to Cu. This indicates that both pure Mg atom clusters and Ag-3Mg co-clusters are difficult to form on $\{111\}_\alpha$ where they would have the largest strain energy if they are formed in the shape of plates. The test "FCC" superstructure for the "quasi-disordered" mixture of Cu and Mg (with ratio1:3) has the lowest strain energy when the co-cluster platelet is parallel with $\{111\}_\alpha$.

3.4 Summary on Clustering Analysis

Both FP-CVM and CALPHAD based on the Q-Chem model were developed for clustering formation analysis prior to the precipitation, and, thereby, the dominating clusters (chemistry of solute aggregates) were predicted in the solid solutions. Strain energy analysis based on FP calculations was used to predict how the clusters are oriented if formed in plate-like shape in the aluminum matrix. From alloy design perspective, the clusters can be classified into the precursor or non-precursors to the desired plate-like 2nd phase. The precursor clusters share, at least partly, the solute elements with and have the same habit planes as the desired 2nd phase. Otherwise, the non-precursor clusters consume the solute contents that are needed for the desired 2nd phase or for its precursor clusters; they may also function as the precursor to the undesired 2nd phases that are deleterious to the desired one.

Applying to the Al-Cu-Mg-(Ag, Si), it was concluded that

a) Cu-rich plate clusters form on {100}, as precursors for θ″ or θ′ {100};
b) Mg and Mg-Ag cannot individually form {111} platelet clusters in Al-Cu-Mg-(Ag), as precursors to desirable Ω (Al2Cu $\{111\}_\alpha$);
c) Certain Mg-Cu (e.g. Mg3Cu and/or Mg-Ag-Cu) clusters tend to form on {111}-habit planes, acting as precursors to Ω;
d) Si forms Mg-Si & Cu-Si clusters, but act as non-precursors;

The clustering analysis potentially provides an effective and efficient tool to identify helpful elements for trace addition and deleterious impurity that must be eliminated, in order to control the competing metastable 2nd phase precipitations.

3.5 Further work on 2nd phase production

Other tasks along this line were either under way or completed when the program ended, and include:

1) To extend the FP-CVM method and to integrate with CALPHAD based Quasi-Chem. The current tetrahedron approximation takes into account only the first neighbor atomic interactions. A pronounced improvement in the resulted free energy as shown in Figure 11 and some other properties including lattice parameters can be expected by considering the second neighbor atomic interactions, *e.g.*, using the octahedron–tetrahedron approximation[49]. While the GGA FP calculations are sufficient to produce consistent cluster energetics, there is still scope for improvement in the pseudopotentials employed. The work employed the site correlation functions to reduce the computational costs.

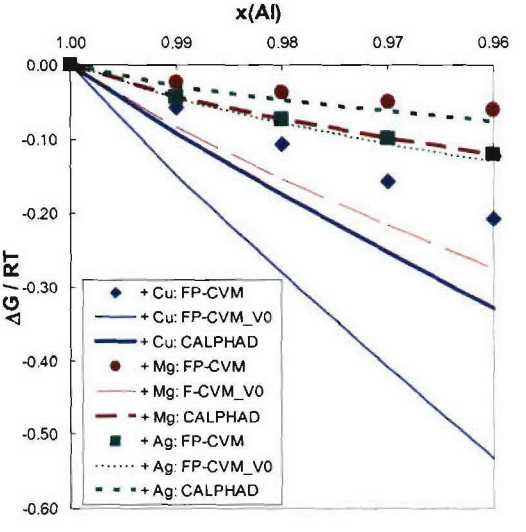

Figure 11 Variation of the free energies of mixing of Al-Cu, Al-Mg and Al-Ag solid solutions obtained by FP-CVM with and without atomic unit-cell compatibility (denoted by the marks and fine lines), by CALPHAD models (denoted by the coarse lines)

2) To examine more elements in order to replace Ag with less expensive elements; such elements may be based on clustering with Mg and Cu for precursors of the desired Ω phase, segregating into the interfaces or partitioning in Ω phase to enhance the coarsening resistance of the Ω precipitates. The preliminary candidate elements were Ni, Cd, Ga, Pd and some rare-earth metals like Ce. Special attention was paid to Ce as some preliminary experiments showed Ce

[28] J.H. Auld, *Acta Cryst.*, 1972, **A28**, S98 Suppl.
[29] S. Kerry and V.D. Scott, *Metals Sci.*, 1984, **18**, 289
[30] K.M. Knowles and W.M. Stobbs, Acta Cryst., 1988, B44, 207.
[31] .C. Muddle and I.J. Polmear, Acta Metall., 1989, 37, 777.
[32] A. Garg and J.M. Howe, Acta Metall., 1991, 39, 1939
[33] Zhu A.W., B.M. Gable, G.J. Shiflet & E.A. Starke, Advanced Materials Engineering, 4, 839 (2003)
[34] Ringer SP, Yeung W, Muddle BC, Polmear IJ, Acta metall. mater. 1994, 42, 1715
[35] C.R. Hutchinson, X. Fan, S.J. Pennycook and G.J. Shiflet, Acta Metall. 2001, 49, 2827
[36] L. Reich, M. Murayama and K. Hono, Acta. Mater., 1998, 46, 17, 6053
[37] Zhu, A. W., Acta Materialia 45, 4213 (1997)
[38] Brook GB, Precipitation in Metals, Special Report No. 3, Fulmer Research Institute: UK, 1963
[39] Sano N, Hono K, Sakurai T and Hirano H, Scripta Metall. Mater. 1991; 25:491
[40] Segall MD, Lindan PLD, M. J. Probert, C. J. Pickard, P. J. Hasnip, S. J. Clark, M. C. Payne, J. Phys.: Cond. Matt. 2002;14(11):2717
[41] Kresse G and Furthmueller J, J. Comput. Mater. Sci., 1996; 6:15
[42] Perdew, J.P.; Burke, K.; Ernzerhof, M, Phys. Rev. Lett. 1996;77:3865
[43] Saunders N and Miodownik AP, CALPHAD-Calculation of Phase Diagrams, Pergamon Materials series v. 1, 1998
[44] Suh IS and Park JK, Scripta metall. mater. 1995; 33:205
[45] Hornstra J and Bartels WJ, J Crys. Growth, 1978; 44:513
[46] Bottomley DJ and Fons P, J. Cryst. Growth 1996; 160, 406
[47] Eshelby JD, Progress in Solid Mechanics 2, eds. I N Sneddon, R Hill, North-Holland, Amsterdam, 1961, p89-140
[48] Lin SCand T Mura T, Phys. Stat. Sol. (a) 1973; 15:281
[49] J.M. Sanchez, F. Ducastelle and D. Gratias, Physica A 128 (1984), p. 334
[50] Meng JC et al, private communication